Environmental Earth Sciences (2018) 77:654
https://doi.org/10.1007/s12665-018-7836-1

ORIGINAL ARTICLE

Dynamic characteristics of tailings reservoir under seismic load

Jiaxu Jin[1] · Chenguang Song[1] · Bing Liang[2] · Yijun Chen[3] · Menglei Su[1]

Received: 19 January 2018 / Accepted: 12 September 2018

Abstract
Earthquake is one of the most important factors that leads to the liquefaction of tailings and to the instability of the tailings reservoir. Therefore, it is of great practical significance to study the instability mechanism of the tailings reservoir under seismic load. In this study, the dynamic characteristics of the tailings reservoir under seismic load were investigated by carrying out a model test on the dynamic characteristics of the tailings dam. A model test of tailings dam failure and the dynamic characteristics model of the tailings reservoir under seismic load were established. Additionally, the dynamic characteristics under a seismic load were investigated. Additionally, the correctness of the dynamic characteristics model of the tailings reservoir was verified by numerical calculation. Researches show that with the increase in input peak acceleration, pore water pressure, earth pressure, and the horizontal and vertical displacements of the dam monitoring points are gradually increased. However, the acceleration amplification factor shows a declining trend. In the process of increasing the input peak acceleration, the saturation line and the lifting speed increases gradually. There is no obvious slip surface in the failure of the tailings dam, and the overall sliding is shown by the failure mode. The tailings reach each of the downstream sections. The mud height increases to the peak value, and then decreases gradually until stagnation. The results of this study can provide the theoretical basis and reference values for the stability analysis of a tailings reservoir under a seismic load, and the results are of great significance for controlling the risk factors in the operation of tailings reservoir, reducing the risk of tailings production safety, preventing the occurrence of tailing pond accidents, protecting the property safety of the downstream residents and enterprises, maintaining social stability around the reservoir area and creating a good ecological environment.

Keywords Tailings reservoir · Seismic load · Dynamic characteristics · Shaking table test · Numerical calculation

Introduction

The tailings reservoir is a major hazard source in metal and nonmetal mines (Papageorgiou et al. 1997; Zhang et al. 2006; He et al. 2009; Özer and Bromwell 2012; Yang et al. 2015). According to the statistical analysis by the World Commission on Dams (ICOLD), since the beginning of twentieth century, more than 200 cases of tailing accidents have been recorded, and most of them are related to earthquakes, since the saturated tailings are prone to liquefaction due to the earthquake, which leads to local dam breaking (Ishihara 1984; Fourie et al. 2001; Wanatowski and Chu 2007; Verdugo and González 2015). Therefore, the instability of the tailings dam has become the center of attention for scholars in various countries (Obermeier 1996; Krinitzsky and Hynes 2002; Fang 2007; Singh et al. 2007; Fell et al. 2007; Huang et al. 2017). Based on the analysis of earthquake damage to the tailings dam, Harper et al. (1992) introduced a seismic evaluation method for a tailings dam. Seid-Karbasi and Byrne (2004) used the commercial software FLAC to analyze the dynamic stability of the Mochikoshi tailings dam, and provided a brief discussion on aseismic measures. Based on the limit equilibrium method and the Mohr Kulun criterion, the problem of seismic liquefaction of the tailings reservoir was investigated and the deformation prediction of the tailings reservoir was carried out by Mayoral and Romo (2008). Ishihara et al. (2015) proposed a simplified method to investigate the water level variation

✉ Chenguang Song
song_chenguang@163.com

[1] Department of Civil Engineering, Liaoning Technical University, Fuxin, China

[2] Department of Mechanics and Engineering, Liaoning Technical University, Fuxin, China

[3] State Key Laboratory of Geomechanics and Geotechnical Engineering, Institute of Rock and Soil Mechanics, Chinese Academy of Sciences, Wuhan, China

Published online: 19 September 2018

of the Mochikoshi tailings dam post-earthquake. Through an indoors experiment and numerical simulation of muddy water seepage, Bu et al. (2016) investigated the mechanism that the deposition of tailing particles in the dam body leads to an increase of the seepage line of the tailings dam, which affected the overall stability of the tailings dam. Most of these studies involved the stability analysis of the tailings dam under static and seepage conditions. However, few studies exist on the dynamic characteristics of the tailings reservoir under seismic load (Psarropoulos and Tsompanakis 2008; Liu et al. 2012), and there have been very few reports on the simulation of tailings dam failure by a shaking table (Chen et al. 2012). In order to reveal the instability mechanism of the tailings reservoir under seismic load, it is necessary to understand the dynamic characteristics of the tailings reservoir (Kossoff et al. 2014; Zhang et al. 2015, 2016; Tang et al. 2017; Xu et al. 2017). Therefore, an investigation on the dynamic characteristics of the tailings reservoir under seismic load has important practical significance in the study of the instability mechanism of the tailings reservoir.

In this work, the variation law of acceleration, pore water pressure, earth pressure, and displacement of the tailings reservoir under seismic load were studied by carrying out a model test with regard to the dynamic characteristics of the tailings dam, and a model test of tailings dam failure. The macro-failure process of the tailings reservoir was recorded by a high-speed camera to discuss the evolution law of mud depth along the dam and the accumulation form in front of the dam after breaking. The instability mechanism of the tailings reservoir under seismic load was analyzed. The research results could provide theoretical basis and reference value for the safe operation of the tailings reservoir, and also have important significance for protecting the safety of residents downstream of tailings reservoirs and for preserving the ecological environment around the reservoir area.

Experimental design

Due to the complex structure of tailings reservoir, many factors need to be considered, it is difficult to carry out field tests and predictive analysis, so the dynamic characteristics of tailings reservoir can only be studied by model test and numerical calculation. In tailings, there is fine layering of coarse and fine materials due to sluiced sand, so the pore water pressure transducers and the piezometric tubes are used to measure the seepage line and pore pressure. The results of the model test can provide a reference for the stability analysis of the actual tailings reservoir engineering though there are some differences between the simulation model and real.

Model test of tailings dam dynamic characteristics

In order to study the dynamic characteristics of the tailings reservoir under seismic load, the dynamic characteristics model test for the tailings reservoir was carried out on a shaking table (Shake Table II-240). Through a dynamic data acquisition system, the dynamic characteristics of the key points of the tailings reservoir model were analyzed. The schematic of the test model box and sensor layout is shown in Fig. 1.

According to the design data, the drainage pipes were embedded, the piezometric tubes were set up, and the initial dam was built by the gravel pile. The tailings slurry was configured according to the actual proportion of 30–40%

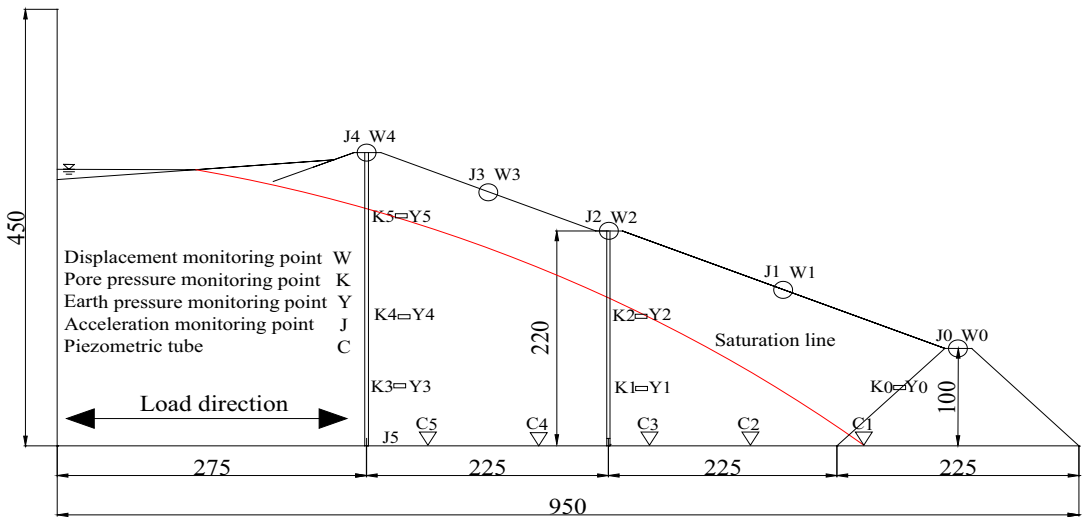

Fig. 1 Schematic of model (unit: mm)

Fig. 2 Front view of model box after stacking

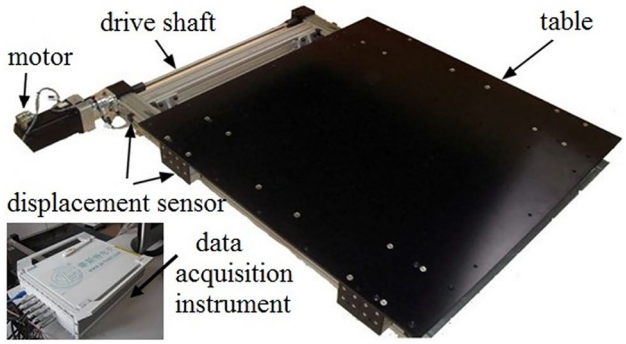

Fig. 3 Shaking table

(weight ratio), and the pulp mixer was used for stirring and pulping. In the upper part of the model box, the slurry discharge pipe was installed, which was used to build the sub-dams, and then the tailings are slowly discharged into the reservoir to complete the accumulation process of the tailings reservoir. The model box was mounted over the shaking table; in the process of dam construction, the tailings sand conveyed to the model box should be compacted to form the sub-dams.

In the process of dam filling, the pin was buried in the tailing sand at a certain distance, and the coordinates of each mark point were recorded. All test instruments were opened, the output acceleration of the shaking table was controlled, and the water level of the piezometric tube was recorded. The front view of the model box after the completion of the stacking dam is shown in Fig. 2. With consideration to seismic response analysis, horizontal waves play a major role in earthquake engineering; therefore, this experiment provided a horizontal seismic wave as a dynamic load input through the shaking table (Fig. 3). Additionally, the selected seismic wave was filtered and the baseline processing was corrected

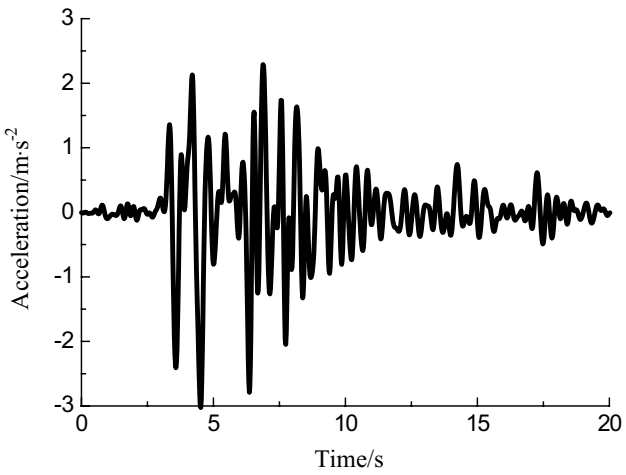

Fig. 4 Seismic waves

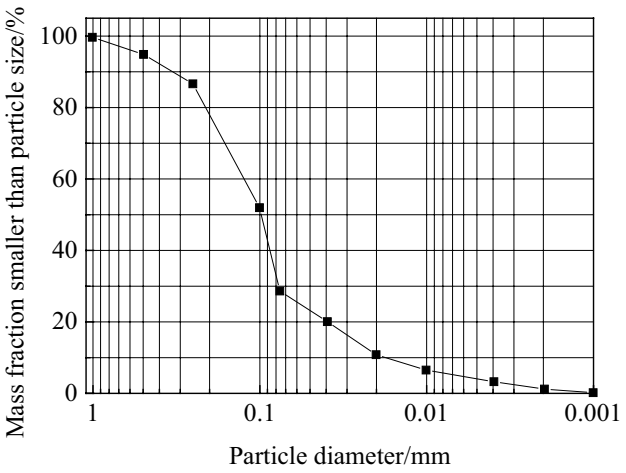

Fig. 5 Particle size distribution (specific grading) curve

by utilizing the SeismoSignal software. The seismic waves of the test were obtained by the above processing and are shown in Fig. 4. The input accelerations in each case were 0.1g, 0.2g, 0.3g, 0.4g, 0.5g, and 0.6g, respectively.

The tailings used in the test were taken from a tailings reservoir in Liaoning, China. The average specific gravity of the tailings sand was 3.03, the field moisture content was 14.9%, the dry density was 1.76g/cm^3, the void ratio was 0.853, the liquid limit was 35.4%, and the plastic limit was 17.8% (Jin et al. 2017a, b). Figure 5 shows the specific grading curve.

Model test of tailings reservoir break

Because the tailings dam break test was destructive, and with consideration to the particularity of the tailings dam itself, the model test can only be used for investigation. In

the experiment, the evolution pattern of the tailings mortar after dam breaking was photographed by a camera, the depth and range of the slurry were recorded, and a height measuring ruler was installed downstream in order to measure the change of the slurry flow height.

In this experiment, a frequency of 2 Hz and a 2-mm amplitude sine wave was used to replace the seismic wave, which was convenient for observing the entire process of dam failure. The occurrence of dam failure is often a sudden process after a certain accumulation, but it is difficult to grasp because of the sudden time. Considering that the dam could eventually achieve the dam break under the dynamic loading action, and according to the previous test results, the vibration holding time was selected for 5 min, the input acceleration was 0.3g.

Experimental results and discussion

Analysis of tailings reservoir dynamic characteristics

Acceleration response analysis

The vibration acceleration response was obtained from the acceleration sensor embedded in the model. Figure 6 shows the curves of the acceleration magnification factor with the elevation of the dam. As can be seen from Fig. 6, with the increase of elevation, the acceleration amplification was not obvious, and the peak response of the primary dam crest and sub-dam surface were basically the same. The seismic response at the sub-dam crest was enlarged slightly, but not significantly. The acceleration amplification factor showed a decreasing trend with the increase of input peak acceleration. This phenomenon was related to the increase of the shear strain, decrease of stiffness, and the increase of tailings sand damping (Wang et al. 2010). According to the research results of Song et al. (2016), when the shear strain γ_d increases gradually at the level of 10^{-5}–10^{-3}, no matter it is biaxial consolidation or isobaric consolidation, the curve of damping ratio-shear strain begins to increase, and the tailings sand damping increases. With the increase of input peak acceleration, the tailings sand exhibited obvious nonlinearity, and its filtering effect gradually increased, this resulted in the decrease of acceleration amplification factor.

Pore water pressure analysis

The water level of the piezometric tube that was recorded in the test process is arranged into the variation curve of the saturation line with the input peak acceleration, as shown in Fig. 7. It can be seen from the figure that in the process of gradual increase of input peak acceleration, the saturation line gradually increased. Additionally, the lifting speed increased gradually with the increase of input peak acceleration; when the input peak acceleration reached 0.4g, the reservoir water level reached the highest level of dynamic loading, the sub-dam surface had a small amount of water precipitation, and liquefaction occurred locally in the dam body. Once the input peak acceleration increased again, the height of the saturation line remained unchanged.

Figure 8 shows the peak values of pore water pressure at the monitoring points around the slope face and the inner section of the dam in the case of input acceleration of 0.3g. It can be seen from the figure that the peak value of the pore pressure measured by the monitoring points near the air surface (K0, K2) was smaller than that at the inner section of the dam (K3, K4). However, once liquefied, the tailings dam may cause swamping or piping, and lead to dam damage.

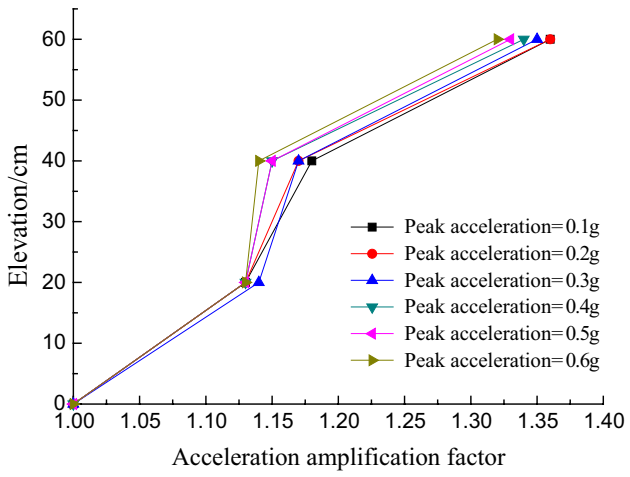

Fig. 6 Graph of acceleration amplification factor with elevation variation

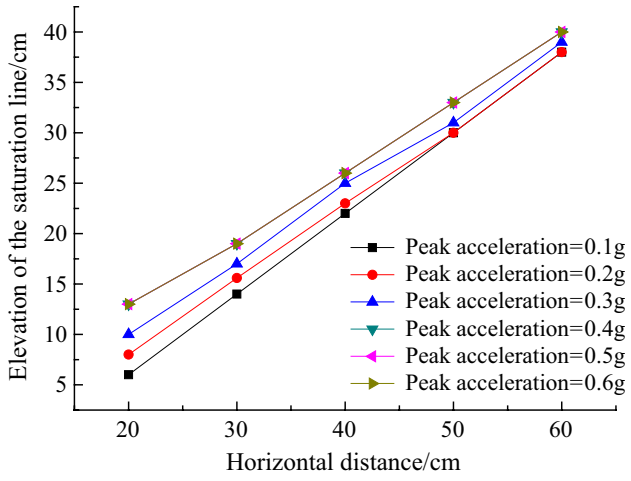

Fig. 7 Curve of the saturation line elevation with the input peak acceleration

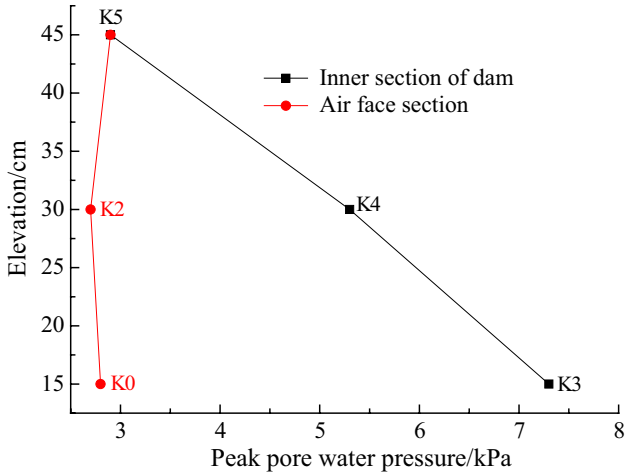

Fig. 8 Graph of pore pressure peak with elevation

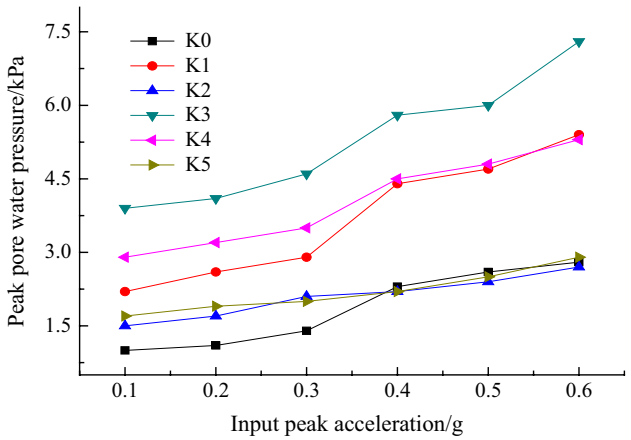

Fig. 9 Graph of pore pressure peak with acceleration peak variation

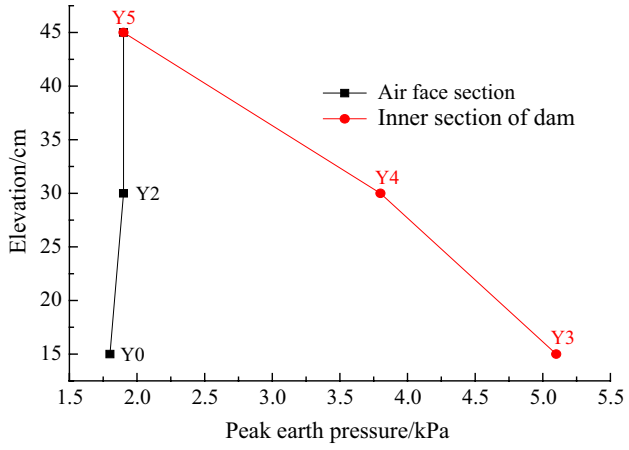

Fig. 10 Graph of earth pressure peak with elevation

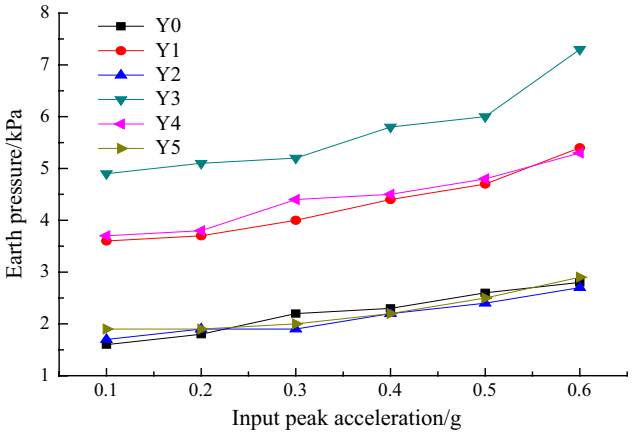

Fig. 11 Graph of earth pressure peak with acceleration peak variation

Figure 9 is the peak value of pore water pressure measured by 6 pore pressure transducers under different input peak acceleration conditions. It can be seen from the figure that the pore water pressure of the dam monitoring points increased with the increase of peak acceleration, and when the input peak acceleration reached 0.4g, the pore water pressure inside the dam basically remained unchanged, which indicated that the tailings had been liquefied. Under dynamic loading, the peak value of pore water pressure in the different positions of the tailings reservoir was different; the pore water pressure of the monitoring points in the lower row were larger, and the pore water pressure of the upper row of the monitoring points was smaller. However, the pore pressure ratio at the bottom row was smaller, and that in the upper row was larger. The pore water pressure inside the slope height was greater than that of the lateral, and the pore pressure ratio was smaller than the lateral pore pressure ratio. This indicated that the tailings sand was easy to liquefy in the air face section.

Earth pressure analysis

Figure 10 shows the peak values of earth pressure at the monitoring points along the slope face and at the inner section of the dam. It can be seen from the figure that the peak value of the earth pressure measured by the 3 monitoring points near the air surface was smaller than that at the inner section of the dam.

Figure 11 is the peak value of the earth pressure obtained by 6 earth pressure sensors under different input peak acceleration conditions. It can be seen from the figure that with the increase of the input peak acceleration, the peak value of the earth pressure of the monitoring point increased gradually.

Displacement analysis

Figures 12 and 13 are displacement curves of the dam surface with dam elevation and peak of input acceleration.

It can be seen from the figure that the horizontal and vertical displacements of the monitoring points of the tailings reservoir are gradually increasing with the increase of input peak acceleration, and that the horizontal displacement of the tailings reservoir was very close to the values when the input acceleration was small (0.1*g* and 0.2*g*). With the increase of input peak acceleration, the horizontal displacement increased greatly, while the vertical displacement increased slightly. This is because the input acceleration was only horizontal acceleration; therefore, the vertical displacement variation was much smaller than the horizontal displacement change. Since the tailings sand was relatively loose and porous, the vertical displacement in the initial stage of the vibration consisted mainly of the consolidation compression of the tailings sand. The displacement of the earlier stage was larger, and the later increment decreased until it finally stabilized during the aftershock.

As can be seen from Fig. 12, for the input seismic wave peak value from 0.1 to 0.2*g*, the horizontal displacement of the tailings reservoir was relatively small, namely, 4 mm and 5 mm, respectively. When the input seismic crest value was from 0.3 to 0.4*g*, the deformation of the dam increased gradually, and the horizontal displacement of the dam crest reached 6 mm and 8 mm, which can be interpreted as the

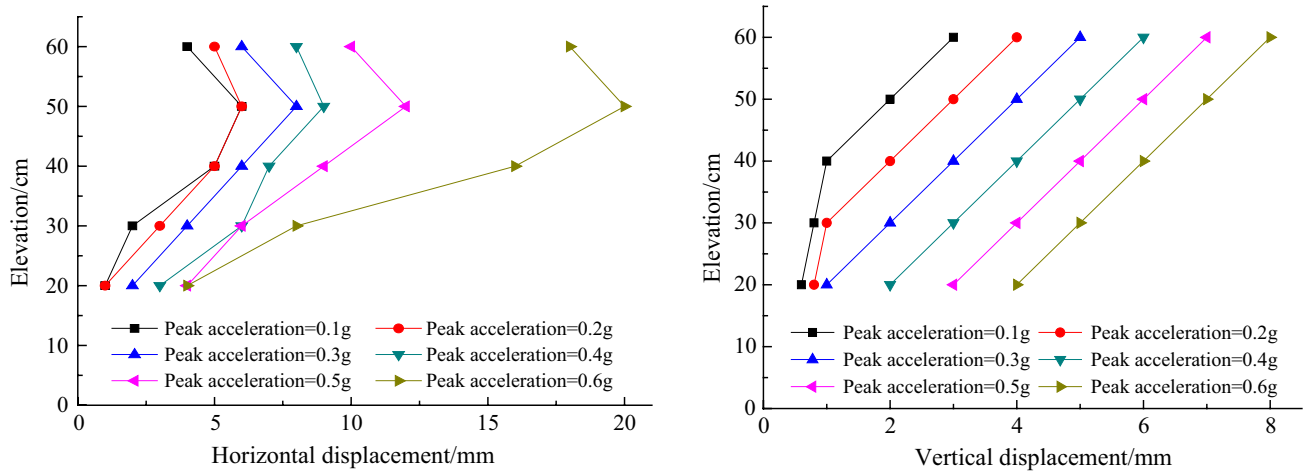

Fig. 12 Displacement curve of dam surface with elevation

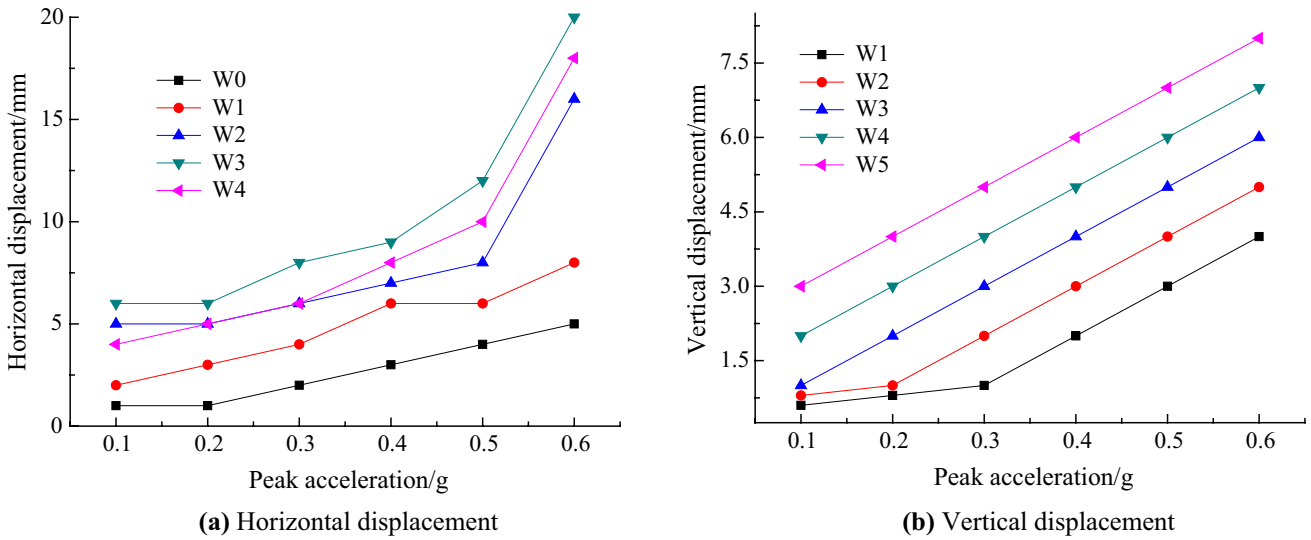

Fig. 13 Displacement curve of dam surface with input peak acceleration

deformation of the dam entering the plastic stage. As can also be seen from Fig. 12, when the peak acceleration was at 0.4g, an inflection point appeared on the curve, which indicated that the tailings dam suffered dynamic failure.

As can be seen from Fig. 13, due to the input acceleration only being horizontal acceleration, the vertical displacement mainly displayed the settlement value of the tailings dam under gravity, as a result of the poor gradation of tailings sand, the porosity of tailings accumulation body being larger, and density being relatively small. Therefore, the displacement of the vertical direction was relatively small under horizontal acceleration.

Dam breaking analysis of the tailings reservoir

Macroscopic analysis of dam failure process and deep mud outburst evolution analysis

The dam failure process of the tailings dam under dynamic loading is shown in Fig. 14. It can be seen from the figure that with the increase of vibration time, the liquefaction of the tailings begun to appear, as shown in Fig. 14a, the water on the surface of the dry beach was precipitated, and the amount of precipitated water was continuously increasing; as the vibration continued for a period of time, the contact area between the two sides of the model and the model box was destroyed. When the vibration continued, the liquefaction range expanded, pore pressure increased, shear strength of tailings sand decreased, sub-dam slipped, and large liquefaction occurred at the dry beach. Figure 14b shows that the failure occurred in the toe of the tailings model. The tailing sand was partially washed out from the lower part of the tailings dam with water, and resulted in the loss of tailings sand. The flow of tailings sand reduced the strength of the dam body. Figure 14c, d shows that the dam collapsed under the dynamic loading action, and the dam slid along the bottom of the dam. According to the existing failure mode, the tailings mortar in the tailings dam model diffused to the downstream after dam failure, and the vertical settlement of the dam crest reached 5 cm.

Through analyzing the mud submergence elevation of the downstream cross section, the variation law of the mud depth time history and the mud evolution law of three typical sections were obtained, as shown in Fig. 15. When the mud reached the downstream cross section, the mud height increased rapidly to its peak value. With the mud evolving downstream, the mud height decreased gradually until the mud was stagnant. The entire mud submergence height

(a) Small amount of water being released from the dry beach

(b) Tailings mortar expanding at the toe of the tailings dam model

(c) Tailings expanding downstream

(d) Crest settlement after stopping vibration

Fig. 14 Macro-figures of dam-breaking process

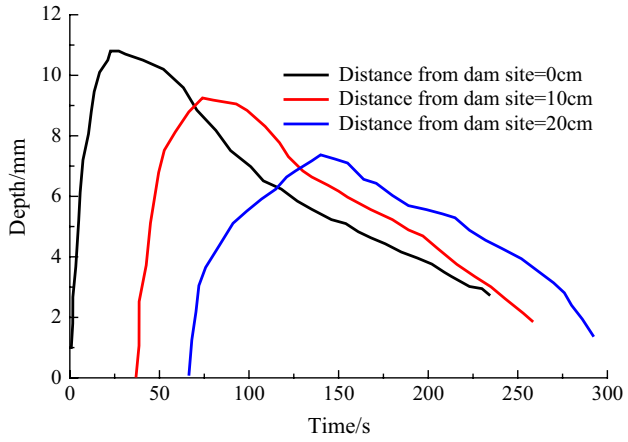

Fig. 15 Deep mud outburst evolution curve

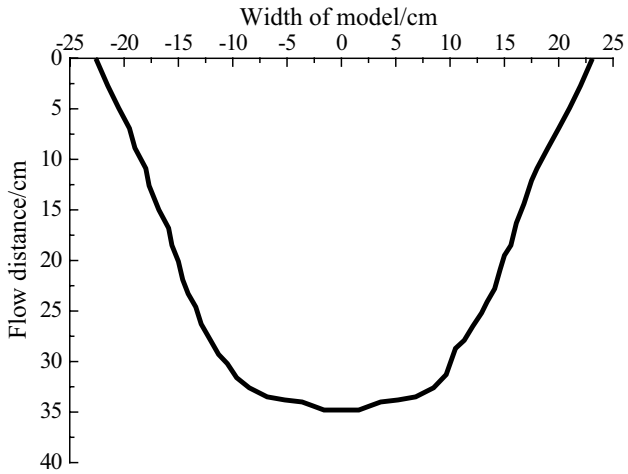

Fig. 16 Cross-sectional shape after dam failure

process line can be generalized into a triangle (Jin et al. 2017a, b).

Accumulation form after dam failure analysis

It can be seen from Fig. 16 that the final accumulation form of the dam was a semi-ellipse. The semi-elliptical long axis was along the direction of the tailings dam. Its short axis was along the direction of the tailings flow, and it was an accumulation fan slightly larger than half of the ellipse. The accumulation thickness of the tailings accumulation fan was thick in the middle, and gradually thinned at both sides to form a certain accumulation slope. The formation of the accumulation slope was caused by the viscosity of the liquid slurry in the tailings mortar and the friction resistance of the solid particles. The accumulation thickness gradually thinned from the front of the dam to the downstream and formed a certain accumulation slope. The final accumulation form of the dam break sand flow was a fan-shaped body with a thick tail and thinned edge. It can be seen from the figure that the maximum vertical submerged distance was 33 cm ahead of the primary dam, and that the maximum horizontal submergence distance of the left and right sides of the primary dam were 22.5 cm and 23 cm, respectively. There is little difference between the two sides of the displacement. The entire figure after dam break was symmetrical along the axis.

Through the model test of the tailings dam failure, it can be seen that the failure of the tailings dam had no obvious slip surface. Most of the dam breaking was due to the increase of tailings pore water pressure in the sub-dam under dynamic loading. The shear strength decreased and liquefaction occurred, which led to dam failure (Djafar Henni et al. 2011; Krim et al. 2013; Bayat et al. 2014). Therefore, the tailings sand in any grade sub-dam could easily lead to the destruction of the dam, when most of the tailings were liquefied.

Analysis of tailings dam instability mechanism under seismic load

Under seismic load, pore water and tailings in the saturated tailings sand move together due to inertia. The pore structure of the saturated tailings sand varied with gravity, and the pore decreased. The pore water of the tailings sand had no movement path for a short time, and could not be dissipated. This made the pore water pressure increase and the effective stress in the tailings sand decrease. When the effective stress of the tailings particles fell to zero, no interactions occurred between particles and the shear strength was reduced to zero. The saturated tailings entered an almost suspended state. This state was obviously different to the ordinary state. In other words, the shape could not be kept unchanged at that moment. From a fluid mechanics viewpoint, this was a typical fluid state. In this fluid state, minor external loads (including gravity and seismic load) will cause tailings to flow. If there was no deformation boundary condition, the flow deformation would develop into an unrestricted flow. In practice, however, the confined boundary conditions existed around any liquefiable site; therefore, the liquefaction site would have large flow deformation, but this would not be an unrestricted flow deformation. When most tailings in the tailings dam were liquefied, the strength of the dam decreased rapidly. The external load passed through the tailings and acted on the sub-dam, which resulted in the movement of tailings to the surface. After a certain displacement, the dam was destroyed, and the tailings sand in the tailings dam flowed out through the destruction of the sub-dam, where it had a huge impact such that the tailings sand at the damage site flowed downstream. The breach was constantly expanding and eventually led to the failure of the dam.

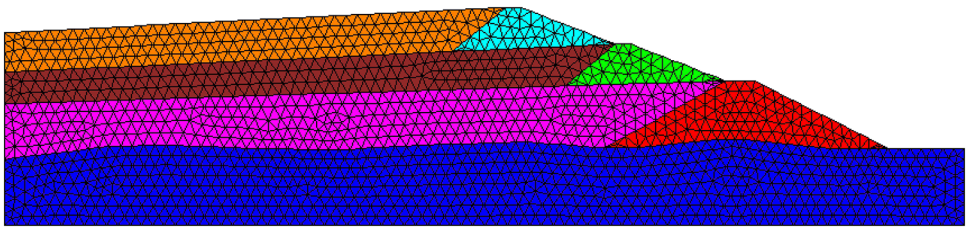

Fig. 17 Numerical simulation model diagram

Table 1 Dynamic parameters of tailings sand (Jin 2014)

Type of tailings sand	Density/kg m^{-3}	Cohesion/kPa	Internal friction angle/°	Dynamic elastic modulus/MPa	Dynamic Poisson's ratio	Dynamic shear modulus/MPa
Primary dam	1780	20	28	201.35	0.41	160.0
Sub-dam	1750	10	30	205.27	0.41	170.0
Tailings sand	1710	10	36	124.57	0.41	44.1
Dam foundation	2400	400	38	500.23	0.38	196.6

The results can be extrapolated to the reality to a certain extent. Due to the difference of the seismic load strength (Ofoegbu et al. 2017; Naeini and Akhtarpour 2018), the dam slope ratio (Shen et al. 2014), the number of sub-dams (Si et al. 2018), and the vegetation protection of the slope surface of the tailings dam (Wang et al. 2018), the results of the paper have some discrepancy with the reality. But on the whole, the instability mechanism of the tailings reservoir under seismic load is the same. In conclusion, a proper design of a tailings dam should be performed on a case-by-case basis to take into consideration the specific local site conditions, apart from the seismological conditions, and the individual characteristics of the dam.

In 2013, the dam break of the tailings reservoir of Jianping JinYuan Mining Co., Ltd. in Jianping County, Liaoning Province, China, was caused by a sudden earthquake. The accumulation form of the dam after the dam break was analyzed in the later period, it was found that the accumulation form of the dam after the dam break was approximately axisymmetric, the maximum longitudinal submergence distance is the same order of magnitude as the results of the paper according to the actual proportion, which had a certain reference value.

Numerical simulation

Through the numerical calculation of tailings dam dynamic characteristics by the model test, the calculation results were compared to the test results, and the correctness of the model was verified. Moreover, the calculation results were compared to the test results, and the correctness of the model was verified. In the numerical calculation, the model in Fig. 1 was imported into ANSYS and divided into grids. Then it was imported into FLAC3D to generate 6,087 nodes and 25,691 units, as shown in Fig. 17. The selection of calculation parameters is shown in Table 1, based on the results of preliminary tests, details of which are provided by Psarropoulos and Tsompanakis (2008) and Liu et al. (2012). The dynamic load is shown in Fig. 4; the input acceleration was 0.3*g*.

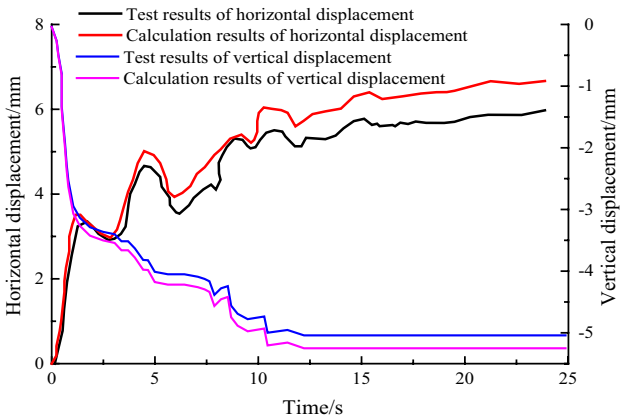

Fig. 18 Contrast of displacement time history curve

The calculation results of the crest displacement were compared to the test results, as shown in Fig. 18. As can be seen from the figure, the calculation results and the experimental results were consistent with the calculation results in the trend. The numerical calculation results were relatively large, in comparison to the test results, with the reason being that, when the test and calculation input the same seismic waveform, the actual acceleration of the table suffers a certain loss due to the impact of the load on the shaking table. That loss is smaller than the numerical value of input acceleration. Moreover, only the plastic deformation part could

not be recovered and the elastic part would recover a little after the action of the seismic wave. From the comparison of the above two methods, it can be seen that the calculated displacement variation law was correct, and that it was suitable for use in subsequent calculation.

Conclusions

1. With the increase of peak acceleration, the acceleration amplification factor decreased slightly; with the increase of dam height, the amplification of seismic acceleration was not obvious, the peak value of the seismic response of the primary dam crest and the sub-dam surface was basically the same, and the seismic response at the sub-dam crest enlarged slightly, but not significantly.
2. Under the dynamic load, the pore water pressure inside the slope height was greater than that of the lateral pore water pressure, and the pore water pressure ratio was smaller than the lateral pore water pressure ratio. This indicated that the tailings sand was easy to liquefy in the air face section. In the normal running state, measures should be taken to speed up the drainage, reduce the water level of the tailings reservoir, enhance the static and dynamic stability of the tailings dam, and ensure the safety and stability of the tailings reservoir under the special conditions.
3. The peak value of the earth pressure measured by the monitoring points near the air surface was smaller than that at the inner section of the dam. With the increase of input peak acceleration, the peak value of the earth pressure of the monitoring point increased gradually.
4. There was no obvious slip surface in the failure of the tailings dam, and the failure mode showed the overall sliding. When the mud reached the downstream cross section, the mud height increased rapidly to its peak value. With the mud evolving downstream, the mud height decreased gradually until the mud was stagnant, and the entire mud submergence height process line could be generalized into a triangle.
5. The results can be extrapolated to the reality to a certain extent. Due to the difference of the seismic load strength, the dam slope ratio, the number of sub-dams, and the vegetation protection of the slope surface of the tailings dam, the results of the paper have some discrepancy with the reality. But on the whole, the instability mechanism of the tailings reservoir under seismic load is the same.

Acknowledgements This research was substantially funded by the National Natural Science Foundation of China (51504123, 51574145), the Natural Science Foundation of Liaoning Province (20170540417), the General Project of the Liaoning Education Department (L2015211), the Innovation Research Fund for Production Technology (20160096T).

References

Bayat M, Bayat E, Aminpour H et al (2014) Shear strength and pore-water pressure characteristics of sandy soil mixed with plastic fine. Arab J Geosci 7(3):1049–1057

Bu L, Zhou H, Li C (2016) Three-dimensional stability analysis of fine grained tailings dam with complex terrain by means of up-stream method. Electron J Geotech Eng 21:3905–3918

Chen G, Wang BH, Sun T (2012) Dynamic shear modulus of saturated Nanjing fine sand in large scale shaking table tests. Chin J Geotech Eng 34(4):582–590

Djafar Henni A, Arab A, Belkhatir M et al (2011) Undrained behavior of silty sand: effect of the overconsolidation ratio. Arab J Geosci 1–11

Fang Y (2007) Some problems in transmitting coefficient method for landslide stability analysis. J Eng Geol 5:005

Fell R, Glastonbury J, Hunter G (2007) Rapid landslides: the importance of understanding mechanisms and rupture surface mechanics. Q J Eng Geol Hydrogeol 40(1):9–27

Fourie AB, Blight GE, Papageorgiou G (2001) Static liquefaction as a possible explanation for the Merriespruit tailings dam failure. Can Geotech J 38(4):707–719

Harper TG, McLeod HN, Davies MP (1992) Seismic assessment of tailings dams. Civ Eng 62(12):64

He Y, Mei F, Shen Z (2009) Analysis of the safety situation and discussion on the management measures of the tailing reservoir. Saf Environ Eng 3:019

Huang Y, Yang Y, Wang L (2017) Evolution of anti-liquefaction performance of foundation soils after dam construction. Bull Eng Geol Environ 2017:1–11

Ishihara K (1984) Post-earthquake failure of a tailings dam due to liquefaction of pond deposit. In: International conference on case histories in geotechnical engineering

Ishihara K, Ueno K, Yamada S et al (2015) Breach of a tailings dam in the 2011 earthquake in Japan. Soil Dyn Earthq Eng 68:3–22

Jin J (2014) Research on dynamic characteristics of upstream tailings under earthquake load. PhD thesis, Northeastern University

Jin J, Cui H, Liang B et al (2017a) Model-based study on collapse of tailings reservoir dam under earthquake action and reinforcement scheme. China Saf Sci J 27(02):92–97 **(in Chinese)**

Jin J, Song C, Chen Y et al (2017b) On the influence of freeze-thaw cycles and moisture content on the mechanical properties of tailings fine sand. J Exp Mech 32(03):431–438 **(in Chinese)**

Kossoff D, Dubbin WE, Alfredsson Met al (2014) Mine tailings dams: characteristics, failure, environmental impacts, and remediation. Appl Geochem 51:229–245

Krim A, el Abidine Zitouni Z, Arab A et al (2013) Identification of the behavior of sandy soil to static liquefaction and microtomography. Arab J Geosci 6(7):2211–2224

Krinitzsky EL, Hynes ME (2002) The Bhuj, India, earthquake: lessons learned for earthquake safety of dams on alluvium. Eng Geol 66(3):163–196

Liu H, Yang C, Zhang C et al (2012) Study on static and dynamic strength characteristics of tailings silty sand and its engineering application. Saf Sci 50(4):828–834

Mayoral JM, Romo MP (2008) Geo-seismic environmental aspects affecting tailings dams failures. Am J Environ Sci 4(3):212

Naeini M, Akhtarpour A (2018) Numerical analysis of seismic stability of a high centerline tailings dam. Soil Dyn Earthq Eng 107:179–194

Obermeier SF (1996) Use of liquefaction-induced features for paleoseismic analysis—an overview of how seismic liquefaction features can be distinguished from other features and how their regional distribution and properties of source sediment can be used to infer the location and strength of Holocene paleo-earthquakes. Eng Geol 44(1–4):1–76

Ofoegbu GI, Dasgupta B, Manepally C et al (2017) Modeling the mechanical behavior of unsaturated expansive soils based on Bishop principle of effective stress. Environ Earth Sci 76(16):555

Özer AT, Bromwell LG (2012) Stability assessment of an earth dam on silt/clay tailings foundation: a case study. Eng Geol 151:89–99

Papageorgiou G, Fourie AB, Blight GE (1997) An investigation of flow failures from breached tailings dams. Eng Geol Environ 3:2477

Psarropoulos PN, Tsompanakis Y (2008) Stability of tailings dams under static and seismic load. Can Geotech J 45(5):663–675

Seid-Karbasi M, Byrne PM (2004) Embankment dams and earthquakes. Int J Hydropower Dams 11(2):96–102

Shen P, Fei W, Liu W et al (2014) Analysis on seismic response spectrum of different slope ratio dam. Adv Mater Res 1092:1341–1345

Si C, Xiong B, Wang W (2018) Analysis on seismic dynamic response and liquefaction area of tailings dam. Int J Comput Appl Technol 57(2):183–191

Singh R, Roy D, Das D (2007) A correlation for permanent earthquake-induced deformation of earth embankments. Eng Geol 90(3):174–185

Song Y, Gao G, Dai Q et al (2016) Experimental analysis on dynamic shear modulus and damping ratio of a mine tailings. Shanxi Arch 42(28):74–76 **(in Chinese)**

Tang Y, Liu Y, Tian J et al (2017) Study on mechanical and chemical properties of tailing soils extracted from one dam site in a cold plateau region. In: Advanced engineering and technology III: proceedings of the 3rd annual congress on advanced engineering and technology (CAET 2016), Hong Kong 22–23 October 2016. CRC, Boca Raton, p 63

Verdugo R, González J (2015) Liquefaction-induced ground damages during the 2010 Chile earthquake. Soil Dyn Earthq Eng 79:280–295

Wanatowski D, Chu J (2007) Static liquefaction of sand in plane strain. Can Geotech J 44(3):299–313

Wang W, Liu B, Zhou Z et al (2010) Equivalent linear method considering frequency dependent stiffness and damping. Rock Soil Mech 31(12):3928–3933 **(in Chinese)**

Wang J, Luo X, Zhang Y et al (2018) Plant species diversity for vegetation restoration in manganese tailing wasteland. Environ Sci Pollut Res 2018:1–10

Xu Z, Yang Y, Chai J et al (2017) Mesoscale experimental study on chemical composition, pore size distribution, and permeability of tailings. Environ Earth Sci 76(20):707

Yang Z, Niu X, Hou K et al (2015) Prediction model on maximum potential pollution range of debris flows generated in tailings dam break. Electron J Geotech Eng 20(11):4363–4369

Zhang X, Wang Q, Xiang G (2006) Analysis of current safety situation of metal and non-metal tailing pond. J Saf Sci Technol 2(2):60–62

Zhang Q, Yin G, Wei Z et al (2015) An experimental study of the mechanical features of layered structures in dam tailings from macroscopic and microscopic points of view. Eng Geol 195:142–154

Zhang P, Hu L, Wu H et al (2016) Mechanical characteristics of mine tailings and seismic responds of tailing reservoir. Jpn Geotech Soc Spec Publ 2(76):2633–2637